Rotation and Translational Motion prior to Self-Assembly: Dynamics of Ethanethiolate on Cu(111)

S. Paterson,* W. Allison, H. Hedgeland, J. Ellis, and A. P. Jardine
The Cavendish Laboratory, JJ Thomson Avenue, Cambridge, CB3 0HE, United Kingdom
(Received 25 March 2011; published 20 June 2011)

We investigate the dynamics of low-coverage ethanethiolate on Cu(111) using helium spin-echo spectroscopy. Above 210 K, the measurements are dominated by translational hopping with an activation energy of only 86 ± 5 meV. At lower temperatures (150–210 K) a further process becomes apparent which has the signature of confined motion. We demonstrate the experimental results are consistent with scattering from an anchored rotor, enabling identification of sixfold jump rotation of the ethyl tail group around a static sulfur adsorption site, with a rotational activation energy of 18 ± 8 meV. Our approach represents a new form of rotational spectroscopy which can be used to study rotational surface diffusion.

DOI: 10.1103/PhysRevLett.106.256101 PACS numbers: 68.35.Ja, 68.35.Fx, 68.43.Jk, 68.49.Bc

The extensive range of potential applications for self-assembled monolayers is now well-known. In particular, the assembly of *n*-alkylthiolates on coinage metal surfaces has generated great interest [1], with aims of developing technologies such as (bio)molecular recognition [2], molecular electronic devices [3], and corrosion inhibiting coatings [4]. Despite this, little is known about the atomic-scale motion involved. In order for molecules to assemble into an ordered structure, both translational and rotational reorientation must occur. Several STM studies have suggested fast motion through observation of ''streaky'' images (e.g., [5]), while others have implied low diffusivities [6]. On Cu(111) and Au(111), low temperature STM has identified sixfold symmetric features, attributed to the rotation of thiols [7–9]. However, the fast time scales involved have prevented quantitative characterization. Elucidation of such dynamic processes is an important step in understanding how systems might be designed to assemble with a desired functionality.

Self-assembly represents a formidable challenge to experiment since it involves the behavior of the isolated molecules as well as interactions between molecular backbones. Here we measure the dynamics of ethanethiolate on Cu(111), a prototypical self-assembling system, at low coverage, where the additional complexity of interactions between molecular backbones may be ignored. These measurements represent the first step in providing a complete description of self-assembly in this system. We establish a general method to identify fast rotational motion. Our results reveal the molecule is highly mobile, well below room temperature. Furthermore, the dominant character changes markedly from translation to rotation as the temperature is reduced. We characterize the dynamics using helium spin-echo spectroscopy (HeSE) [10], an ideal tool with which to study such electron sensitive systems [11]. The unique abilities of HeSE are now established [10,12]. The method provides direct measurement of surface correlations, in both position and time, through the well-known intermediate scattering function (ISF), $I(\Delta\mathbf{K}, t)$ [13], which is related to the van Hove pair correlation function $G(\mathbf{r}, t)$ by a spatial Fourier transform [14]. Each measurement of $I(\Delta\mathbf{K}, t)$ gives the decay in surface correlation with time, t (ps range), and $\Delta\mathbf{K}$, where the latter bears a reciprocal relationship $(2\pi/\Delta\mathbf{K})$ with periodicity in real space. The variation of $I(\Delta\mathbf{K}, t)$ with $\Delta\mathbf{K}$ reveals details of the microscopic dynamics. By extending the application of HeSE to include rotation, we allow determination of rotational activation energies and a more complete description of adsorbate motion.

Above ~140 K ethanethiol deprotonates to the corresponding thiolate upon adsorption [15]. Structural STM and LEED investigations into ethanethiolate on Cu(111) have noted the presence of several different phases, the proportions of which vary with adsorption conditions. Density-functional theory indicates a threefold hollow adsorption site [16], though STM data [5] also suggest bridge site occupation. At higher temperatures, adsorbed thiolates can cause reconstruction of the uppermost Cu layer [1,5,6,11,17,18]. Here we focus on low coverages and temperatures, where we expect the surface geometry to remain well defined.

In the presence of uncorrelated translation and rotation, $I(\Delta\mathbf{K}, t)$ may be written as a product [19],

$$I(\Delta\mathbf{K}, t)_{\text{total}} = I(\Delta\mathbf{K}, t)_{\text{trans}} I(\Delta\mathbf{K}, t)_{\text{rot}}. \quad (1)$$

Translation is well understood [20], and in bulk materials, rotation has been studied by incoherent neutron scattering [21,22], but no models for coherent scattering from a rotating surface species have been proposed. We derive the HeSE signature for rotational jump diffusion by extending an analytic model by Barnes [21], first applied to neutron scattering. Our method is summarized here while more detail is given in the supplemental material [12].

The thiolate is modeled by two equally weighted scattering centers representing the sulfur ''head'' and alkyl ''tail'' [Fig. 1(inset)] [23]. Six preferred orientations of

the alkyl tail group around a sulfur-metal anchor are allowed, as suggested in STM studies [7–9]. A 6×6 tridiagonal matrix is used to represent hopping from site i to an adjacent site j during a time δt. Obtaining the eigenvalues of this matrix enables the probability, P_{ij}, of hopping from i to any site j to be written as [21]

$$P_{ij}(t) = \frac{1}{N} \sum_{k=1}^{N} e^{-t/\tau_\kappa} \cos\left(\frac{2\pi k(i-j)}{N}\right), \quad (2)$$

where $1/\tau_\kappa = 4\beta \sin^2(\pi k/N)$ and N is the number of sites around a circle. β is a rate constant such that the probability of hopping, $p = \beta\delta t$, as $\delta t \to 0$, which is expected to follow an Arrhenius form, $\beta = \beta_0 \exp(-E_r/k_B T)$. Barnes obtains $I(\Delta\mathbf{K}, t)$ in the powder average limit. However, for comparison with HeSE experiments, we wish to preserve azimuthal information. Substituting (2) into the definition of the self part of $I(\Delta\mathbf{K}, t)$ [13] and summing over all the equivalent initial and final sites, on a circle of radius r, gives

$$I_{\text{self}}(\Delta\mathbf{K}, t) = \sum_i^N \sum_j^N P_{ij}(t) e^{\{i\Delta\mathbf{K}\cdot[\mathbf{r}_i(t) - \mathbf{r}_j(t)]\}}, \quad (3)$$

which represents the effect of the tail group. We can neglect correlations between different species in the low-coverage limit; however, since helium scattering is coherent, it is essential to include correlations between scatterers within the same species. A further summation includes the head group as a stationary particle at the origin [13].

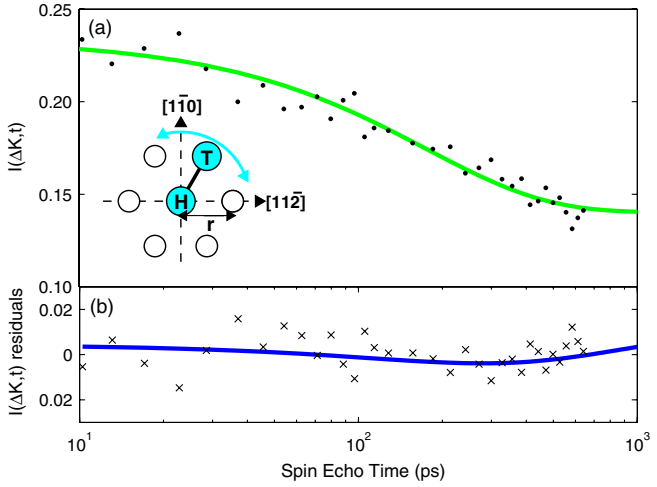

FIG. 1 (color online). (a) is an example of a typical measured ISF (black points) for ethanethiolate on Cu(111) at 150 K ([11$\bar{2}$], $\Delta\mathbf{K} = 0.67$ Å^{-1}) fitted with a single exponential function (green line). (b) shows the residuals between the data and single exponent (black crosses), compared with the deviation between the single exponential and model rotational ISF (blue line), demonstrating the deviation between models lies well within the noise of the data. The inset illustrates the model geometry for a thiolate species, comprising head (H) and tail (T) groups on a sixfold lattice. A tail scatterer at site i may hop to $i + 1$ or $i - 1$ around the anchored head.

We thus obtain a model for scattering from our rotor species, of the form

$$I(\Delta\mathbf{K}, t)_{\text{rot}}^{11\bar{2}} = C_1 e^{-\beta t} + C_2 e^{-3\beta t} + C_3 e^{-4\beta t} + C_4, \quad (4)$$

$$I(\Delta\mathbf{K}, t)_{\text{rot}}^{1\bar{1}0} = C_5 e^{-\beta t} + C_6 e^{-3\beta t} + C_7, \quad (5)$$

which represent, respectively, scattering aligned with one of the molecular axes [11$\bar{2}$], or midway between the molecular axes [1$\bar{1}$0]. Coefficients C_1 to C_7 are known periodic functions of both $\Delta\mathbf{K}$ and r [12]; however, β is independent of momentum transfer. Note that, as $t \to \infty$, the ISF decays to a nonzero limit (C_4 and C_7 in the respective directions), which is a key signature of confined motion. A stationary anchor does not affect the dephasing rate, but does determine the $\Delta\mathbf{K}$ and r dependence of C_4 and C_7.

Experimental measurements were carried out using the Cambridge HeSE spectrometer. A single crystal Cu(111) sample (Surface Prep. Lab., NL) was mounted and prepared by repeated cycles of Ar^+ sputtering (800 eV, 300 K) and annealing (800 K, 30 s), until helium reflectivity measurements confirmed a high surface quality. Ethanethiol (Sigma Aldrich, 97%) was purified by repeated freeze-pump-thaw cycles, before dosing the sample (held at 150 K) by backfilling the chamber to $\sim 2 \times 10^{-8}$ mbar. Surface uptake was followed using the specular helium signal, to achieve an estimated coverage of 0.03 ML, measured by assuming an effective cross section of 100 Å^2 [25]. HeSE measurements were taken between 150 K and 325 K and at $\Delta\mathbf{K} = 0$–2.5 Å^{-1} along the [1$\bar{1}$0] and [11$\bar{2}$] azimuths.

Figure 1(a) shows a typical 150 K measurement which we will later show corresponds to rotation. The loss of surface correlation is evident through a decrease in $I(\Delta\mathbf{K}, t)$ on a characteristic time scale of a few hundred picoseconds. We attribute this observation to a highly mobile ethanethiolate species, as measurements on a clean Cu(111) surface show no decay. Simple diffusion models, where $I(\Delta\mathbf{K}, t)$ decays exponentially, give a single decay constant or "dephasing rate," α, to be acquired from each measurement. The shape of $\alpha(\Delta\mathbf{K})$ characterizes the mechanism of the motion, while its magnitude gives the absolute rate [10]. The form of our rotational model [Eqs. (4) and (5)] differs fundamentally from that of simple diffusion, in that the variation in dephasing rate with $\Delta\mathbf{K}$ is due to the change in the relative magnitudes of the pre-exponential factors (C_1 to C_7). However, the resulting shape of $I(\Delta\mathbf{K}, t)_{\text{rot}}$ remains similar to a simple exponential. In Fig. 1(b) the residuals between the rotational data and a single exponent (crosses) are compared with those between the same single exponential and the model rotational ISF (blue line). The deviation between the model and a single exponential is negligible and much smaller than the noise in the data. Our approach, therefore, is to extract an effective dephasing rate, α_{eff}, using a single exponential to describe and compare both the data and the rotational model.

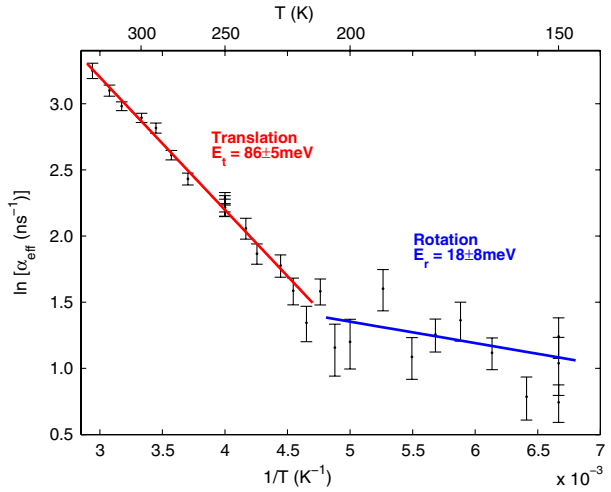

FIG. 2 (color online). Arrhenius plot of the dephasing rate of ethanethiolate on Cu(111), along the [11$\bar{2}$] azimuth at $\Delta\mathbf{K} = 0.47$ Å^{-1}. A striking change in activation energy of the dynamical process is observed at approximately 210 K. The fast motion at 210–325 K is attributed to translational jumps, whereas weakly activated rotation is apparent at 150–210 K.

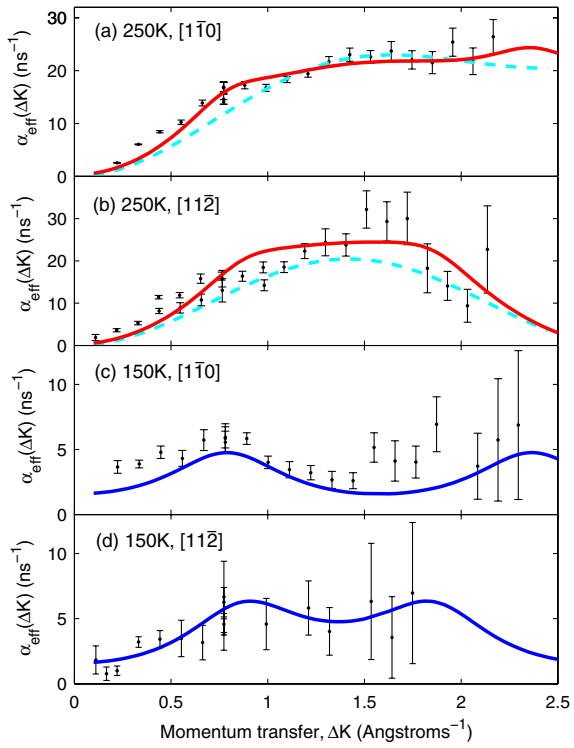

FIG. 3 (color online). (a) and (b) show the measured $\alpha_{\text{eff}}(\Delta\mathbf{K})$ variation for ethanethiolate at 250 K (black points) which resembles the Chudley-Elliott [20] model for single hops of one lattice spacing along [1$\bar{1}$0] (cyan dashes). A closer fit to the data is obtained using a combined model of rotation and translational hops (solid red lines). (c) and (d) show 150 K measurements (black points) with the signatures for discrete rotation on a sixfold lattice, determined from our analytic model (solid blue lines) where $r = 4.6 \pm 0.3$ Å^{-1} and $\beta = 1.6 \pm 0.3$ ns^{-1}.

Figure 2 shows the temperature dependence of the effective dephasing rate for data acquired at $\Delta\mathbf{K} = 0.47$ Å^{-1} along [11$\bar{2}$]. The change in slope of the Arrhenius plot indicates two regimes with distinctly different activated processes and a transition at ~210 K. There are corresponding changes in the $\Delta\mathbf{K}$ dependence of the effective dephasing rate, as shown in Fig. 3. Figures 3(a) and 3(b), at 250 K, show the high temperature regime and 3(c) and 3(d), at 150 K, the low temperature regime. Taken together these observations indicate that the dominant character of the motion changes between high and low temperature. At high temperatures [Figs. 3(a) and 3(b)] the observations have the characteristic of two-dimensional translational motion [20], as shown by the analytic model for single hops along [1$\bar{1}$0] and [11$\bar{2}$], respectively (cyan dashes) [26]. Note, in particular, that $\alpha \rightarrow 0$ as $\Delta\mathbf{K} \rightarrow 0$. This behavior contrasts with the low temperature data [Figs. 3(c) and 3(d)] where the $\Delta\mathbf{K} \rightarrow 0$ limit and the $\Delta\mathbf{K}$ dependence are those expected from the model of rotationally confined motion described above (solid blue lines). The two parameters in the rotational model were obtained by fitting the $\alpha_{\text{eff}}(\Delta\mathbf{K})$ data at 150 K, giving $\beta = 1.6 \pm 0.3$ ns^{-1} and $r = 4.6 \pm 0.3$ Å. The radius, r, is consistent with the enlarged cross sections typical of He scattering experiments and, as such, should be regarded as an *effective* size. While the activation energy for the translation dominated, high temperature regime can be extracted directly from the gradient of the Arrhenius plot, this is not the case for lower temperatures, due to the more complex form of $I(\Delta\mathbf{K}, t)$. We instead calculate $E_r = 18 \pm 8$ meV by optimizing the rotation model to reproduce the 150–210 K Arrhenius results (Fig. 2). We have investigated other geometries including threefold and fourfold jump rotation (due to possible reconstruction [11]), different azimuthal orientations, and continuous rotation. However these give very different dynamical signatures [27]. Other forms of confinement such as perpendicular motion [28] or intracell motion [29] may be ruled out as the form and intensity of the decaying signal are not consistent with the data.

A more complete representation of the adsorbate dynamics is obtained when rotational and translational processes occur concurrently, but with different levels of thermal activation. The solid lines in Figs. 3(a) and 3(b) show translation combined with the rotation model which best represented the 150 K measurements [using Eq. (1)]. $\beta(T)$ was scaled according to our measured activation energy to give $I(\Delta\mathbf{K}, t)_{\text{rot}}$. The inclusion of rotation provides an improved description of the 250 K data [Figs. 3(a) and 3(b)], confirming our interpretation. Since each ISF is interpreted using a single exponential, one process generally dominates, leading to the clear change of slope in Fig. 2. Near 300 K, the decay in $I(\Delta\mathbf{K}, t)$ is mainly due to translation but with a small rotational contribution, whereas, at 150 K, translational hops are sufficiently infrequent that only rotation is evident.

Approximate diffusion constants for the high temperature region can be obtained in the long length scale

limit (small $\Delta\mathbf{K}$). Taking $\alpha = D\Delta\mathbf{K}^2$, gives $D = D_0 \exp(-E_a/k_B T)$ where the diffusion constant is $D_0 = 2.2 \pm 0.2 \times 10^{-4}$ cm^2/s. These rates are high compared to those for atomic sulfur [30], indicating the alkyl chain dramatically alters the lateral adsorbate-substrate potential energy surface.

Overall, reproduction of the features in the $\alpha_{\mathrm{eff}}(\Delta\mathbf{K})$ data, as well as the general quality of fit, gives strong support to a sixfold jump rotational process at low temperatures. Evidently rotation plays an important role in the dynamics of this system, and clearly, ethanethiolate is rotationally active well before the onset of translation.

Our measurements suggest preferential orientation of ethanethiolate along the $[11\bar{2}]$ axes, which indicates atop-site adsorption. Theoretical work suggests that upon thiol deprotonation, the top site reverts from most to least favorable [31,32]; however, these calculations were carried out at much higher coverages. If we assume hollow-site adsorption [16], with a local threefold symmetry, preferred sixfold orientation along $[11\bar{2}]$ can only be explained if there were an unusually long-range interaction between the alkyl chain and the surrounding Cu lattice.

It is possible that the behavior of thiolate/Au(111) systems, whereby molecules adsorb on and diffuse with adatoms [33], may also be exhibited on Cu(111). While our measurements cannot directly confirm or exclude this possibility, we anticipate that knowledge of a measured activation energy will provide a stringent test of future theoretical models aiming to resolve this issue fully.

In summary, we have presented the first data describing the dynamical behavior of thiolates on a copper surface, a key step towards full elucidation of the self-assembly process. We have established fast translational diffusion, accompanied by rotational reorientation. Our work represents a new class of measurement, acquiring information on surface rotational dynamics of systems in thermal equilibrium. It is increasingly evident that rotation, along with other forms of higher dimensionality [34,35], plays a key role in determining the mechanism of atomic-scale motion and more complex assembly processes. We therefore anticipate that our approach, which in principle enables a complete statistical description of fast (picosecond) aperiodic rotational and translational surface motion, may be of rather general application.

*sp552@cam.ac.uk

[1] D. P. Woodruff, Phys. Chem. Chem. Phys. **10**, 7211 (2008).

[2] F. J. Schmitt, L. Haussling, H. Ringsdorf, and W. Knoll, Thin Solid Films **210-211**, 815 (1992).

[3] A. M. Moore, A. A. Dameron, B. A. Mantooth, R. K. Smith, D. J. Fuchs, J. W. Ciszek, F. Maya, Y. X. Yao, J. M. Tour, and P. S. Weiss, J. Am. Chem. Soc. **128**, 1959 (2006).

[4] F. P. Zamborini and R. M. Crooks, Langmuir **13**, 122 (1997).

[5] S. M. Driver and D. P. Woodruff, Langmuir **16**, 6693 (2000).

[6] M. Laurin, X. Shao, Y. Fujimori, A. Nojima, E. O. Sako, J. Miyawaki, M. Shimojo, Y. Iwasawa, T. Ohta, and H. Kondoha, J. Electron Spectrosc. Relat. Phenom. **172**, 88 (2009).

[7] B. V. Rao, L. Bartels, and A. W. Liu, Chem. Phys. Lett. **385**, 36 (2004).

[8] B. V. Rao, K. Y. Kwon, A. W. Liu, and L. Bartels, J. Chem. Phys. **119**, 10 879 (2003).

[9] J. Cho, N. Levy, A. Kirakosian, M. J. Comstock, F. Lauterwasser, J. M. J. Frechet, and M. F. Crommie, J. Chem. Phys. **131**, 034707 (2009).

[10] A. P. Jardine, H. Hedgeland, G. Alexandrowicz, W. Allison, and J. Ellis, Prog. Surf. Sci. **84**, 323 (2009).

[11] S. M. Driver and D. A. King, Surf. Sci. **601**, 510 (2007).

[12] See supplemental material at http://link.aps.org/supplemental/10.1103/PhysRevLett.106.256101 for further details of the spin-echo technique and rotation model.

[13] G. L. Squires, *Introduction to the Theory of Thermal Neutron Scattering* (Cambridge University Press, Cambridge, England, 1978), Chap. 4.

[14] L. Van Hove, Phys. Rev. **95**, 249 (1954).

[15] G. J. Jackson, D. P. Woodruff, R. G. Jones, N. K. Singh, A. S. Y. Chan, B. C. C. Cowie, and V. Formoso, Phys. Rev. Lett. **84**, 119 (2000).

[16] A. Ferral, E. M. Patrito, and P. Paredes-Olivera, J. Phys. Chem. B **110**, 17 050 (2006).

[17] D. P. Woodruff, Appl. Surf. Sci. **254**, 76 (2007).

[18] H. Grönbeck, J. Phys. Chem. C **114**, 15 973 (2010).

[19] R. Hempelmann, *Quasielastic Neutron Scattering and Solid State Diffusion* (Oxford Science Publications, Oxford, 2000), Chap. 5.

[20] C. T. Chudley and R. J. Elliott, Proc. Phys. Soc. London **77**, 353 (1961).

[21] J. D. Barnes, J. Chem. Phys. **58**, 5193 (1973).

[22] M. Bee, *Quasielastic Neutron Scattering* (IOP Publishing, Bristol, 1988).

[23] Despite the extended cross sections of adsorbates in helium-scattering measurements, the treatment of atoms and molecules as point scatterers has been shown to model surface dynamical scattering remarkably well [24].

[24] A. Alderwick, Ph.D. thesis, University of Cambridge, 2009.

[25] D. Farias and K. H. Reider, Rep. Prog. Phys. **61**, 1575 (1998).

[26] We also see a trend of increasing jump length with temperature (not shown).

[27] S. Paterson and A. P. Jardine (to be published).

[28] G. Alexandrowicz, A. P. Jardine, H. Hedgeland, W. Allison, and J. Ellis, Phys. Rev. Lett. **97**, 156103 (2006).

[29] A. P. Jardine, J. Ellis, and W. Allison, J. Chem. Phys. **120**, 8724 (2004).

[30] B. J. Hinch, J. W. M. Frenken, G. Zhang, and J. P. Toennies, Surf. Sci. **259**, 288 (1991).

[31] M. Konopka, R. Rousseau, I. Stich, and D. Marx, Phys. Rev. Lett. **95**, 096102 (2005).

[32] Y. Akinaga, T. Nakajima, and K. Hirao, J. Chem. Phys. **114**, 8555 (2001).

[33] P. Maksymovych, O. Voznyy, D. B. Dougherty, D. C. Sorescu, and J. T. Yates, Prog. Surf. Sci. **85**, 206 (2010).

[34] E. H. G. Backus, A. Eichler, A. W. Kleyn, and M. Bonn, Science **310**, 1790 (2005).

[35] G. Alexandrowicz, A. P. Jardine, P. Fouquet, S. Dworski, W. Allison, and J. Ellis, Phys. Rev. Lett. **93**, 156103 (2004).